

108  
8-1-78

44. 311

ORNL/TM-6302

**MASTER**

**Analysis of Particle Species Evolution  
in Neutral Beam Injection Lines**

J. Kim  
H. H. Haselton

**OAK RIDGE NATIONAL LABORATORY**  
OPERATED BY UNION CARBIDE CORPORATION FOR THE DEPARTMENT OF ENERGY

Contract No. W-7405-eng-26

FUSION ENERGY DIVISION

RECEIVED  
JUL 11 1978

ANALYSIS OF PARTICLE SPECIES EVOLUTION  
IN NEUTRAL BEAM INJECTION LINES

J. Kim and H. H. Haselton

Date Published - July 1978

**NOTICE**  
This report was prepared as an account of work sponsored by the United States Government. Neither the United States nor the United States Department of Energy, nor any of their employees, nor any of their contractors, subcontractors, or their employees, makes any warranty, express or implied, or assumes any legal liability or responsibility for the accuracy, completeness, or usefulness of any information, apparatus, product, or process disclosed, or represents that its use would not infringe privately owned rights.

**NOTICE** This document contains information of a preliminary nature. It is subject to revision or correction and therefore does not represent a final report.

Prepared by the  
OAK RIDGE NATIONAL LABORATORY  
Oak Ridge, Tennessee 37830  
operated by  
UNION CARBIDE CORPORATION  
for the  
DEPARTMENT OF ENERGY

RECEIVED  
JUL 11 1978

## CONTENTS

ABSTRACT . . . . .	v
1. INTRODUCTION . . . . .	1
2. BEAM SPECIES CHANGE IN GAS CELL . . . . .	1
3. CALCULATIONS OF SPECIES EVOLUTION . . . . .	9
4. CALCULATIONS OF NEUTRAL BEAM POWER . . . . .	18
5. CONCLUSIONS . . . . .	20
ACKNOWLEDGMENT . . . . .	20
REFERENCES . . . . .	21

## ABSTRACT

Analytic solutions to the rate equations describing the species evolution of a multispecies positive ion beam of hydrogen due to charge exchange and molecular dissociation are derived as a function of the background gas ( $H_2$ ) line density in the neutralizing gas cell and in the drift tube. Using the solutions, calculations are presented for the relative abundance of each species as a function of the gas cell thickness, the reionization loss rates in the drift tube, and the neutral beam power as a function of the beam energy and the species composition of the original ion beam.

## 1. INTRODUCTION

In neutral beam injectors in use for heating fusion plasmas, a multi-species hydrogen beam (i.e.,  $H_1^+$ ,  $H_2^+$ , and  $H_3^+$ ) from a source undergoes atomic collision reactions in a gas cell and then is separated magnetically or electrostatically into charged particles and neutral particles. The energetic neutral particles travel further downstream and to the fusion plasma, while the charged particles are either dumped into a target or possibly recovered in the form of current by one of several possible techniques. Atomic processes in the gas cell involving charge transfer and dissociation will change particles' charge state and momentum. These processes will determine the species evolution along the gas cell downstream and the neutralization efficiency. The pure neutral particle beam entering the drift tube will also encounter residual hydrogen molecules, and similar atomic processes will determine the reionization losses.

Numerical calculations of this problem have been reported in the literature.<sup>1,2</sup> Although the same problem is considered here, we offer in addition the functional forms of variation with the gas cell thickness for all the species. Furthermore, the detailed information of the fractions of charged particle species arriving at the species analyzer in the ion dump became warranted for use in unfolding the species measurement data obtained at the ion dump into the species distribution of the original ion beam. The functional forms may also be used for the study of the space charge propagation in the gas cell. We also present a calculation of the neutral beam injector efficiency as a function of the beam energy and the species composition for the fixed ion beam current.

## 2. BEAM SPECIES CHANGE IN GAS CELL

Reactions responsible for changing the abundance of each beam species are illustrated in Fig. 1 for three different original ion species,  $H_1^+$ ,  $H_2^+$ , and  $H_3^+$ . In evolution these species are independent of each other. The  $H^-$  species is included in the atomic ion ( $H_1^+$ ) family but neglected in the evolution of molecular ion families for simplicity of analysis (justified by its small net production rate in comparison with other species). We then write the rate equations for the particle densities of species normalized to the one of the original ion species of each family as follows:

**BLANK PAGE**

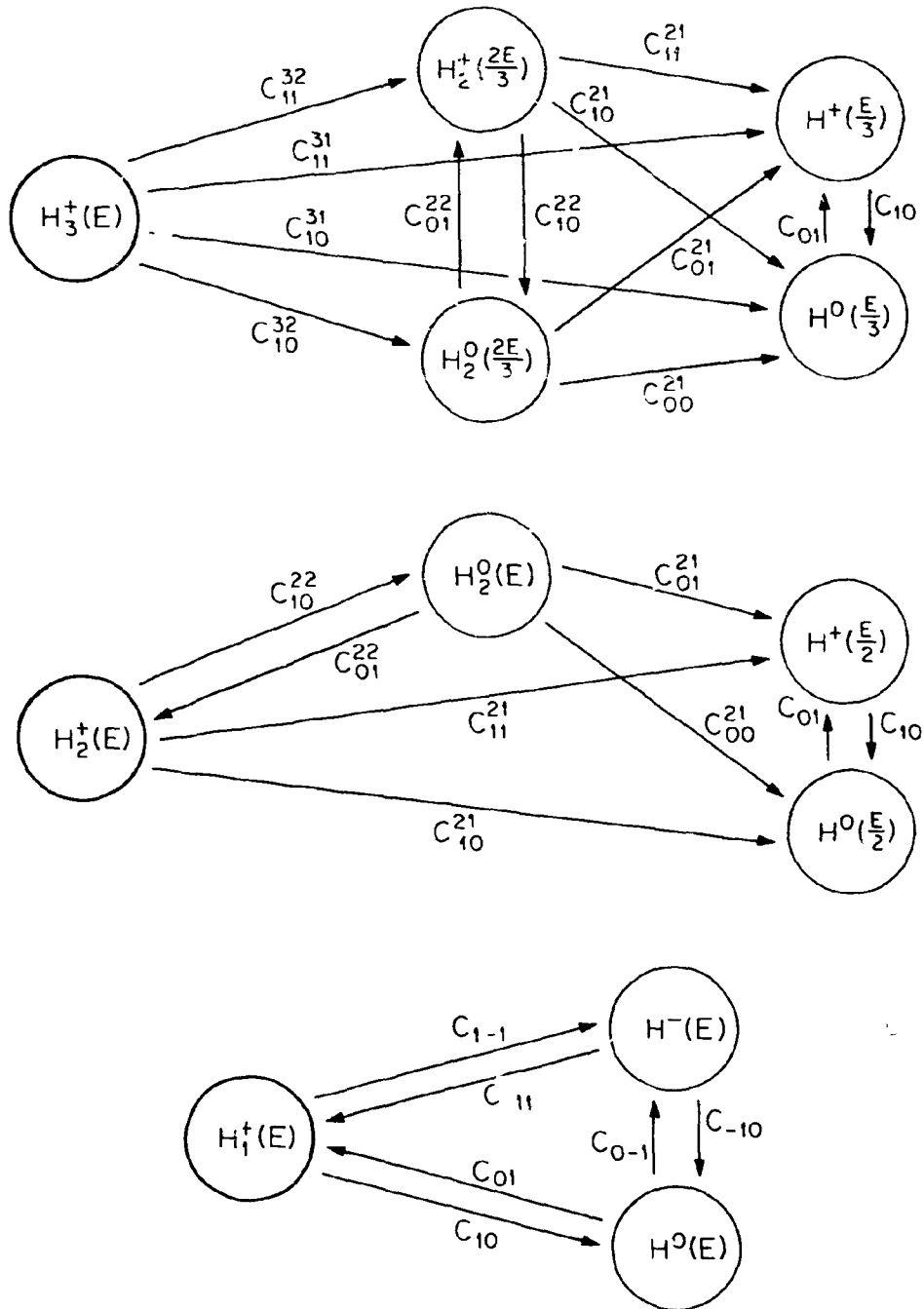


Fig. 1. Reactions altering charge states and momenta of particles for each family originating from  $H_1^+$ ,  $H_2^+$ , and  $H_3^+$ .  $E$  is the original ion beam energy, and  $C_{cd}^{ab}$  denotes the reaction cross section involving a mass change from  $a$  to  $b$  and a charge state change from  $c$  to  $d$ .

H<sub>1</sub><sup>+</sup> family

$$\frac{dy_0}{dx} = -(C_{01} + C_{0-1})y_0 + C_{10}y_+ + C_{-10}y_-$$

$$\frac{dy_+}{dx} = -(C_{10} + C_{1-1})y_+ + C_{01}y_0 + C_{-11}y_- \quad (1)$$

$$y_- = 1 - y_0 - y_+$$

H<sub>2</sub><sup>+</sup> family

$$\frac{dy_{20}}{dx} = C_{10}^{22}y_{2+} - S_5y_{20}$$

$$\frac{dy_{2+}}{dx} = C_{01}^{22}y_{20} - S_4y_{2+} \quad (2)$$

$$\frac{dy_0}{dx} = C_{10}^{21}y_{2+} + C_{00}^{21}y_{20} + C_{10}^{11}y_+ - C_{01}^{11}y_0$$

$$y_+ = 2 - y_0 - 2(y_{20} + y_{2+})$$

H<sub>3</sub><sup>+</sup> family

$$\frac{dy_{3+}}{dx} = -S_3y_{3+}$$

$$\frac{dy_{20}}{dx} = C_{10}^{32}y_{3+} + C_{10}^{22}y_{2+} - S_1y_{20}$$

$$\frac{dy_{2+}}{dx} = C_{11}^{32}y_{3+} + C_{01}^{22}y_{20} - S_2y_{2+} \quad (3)$$

$$\frac{dy_0}{dx} = C_{10}^{31}y_{3+} + C_{10}^{21}y_{2+} + C_{00}^{21}y_{20} + C_{10}^{11}y_+ - C_{01}^{11}y_0$$

$$y_+ = 3 - y_0 - 2y_{20} - 2y_{2+} - 3y_{3+}$$



where

$$x = \text{the line density (cm}^{-2}\text{)}; x = \int_0^{\ell} \rho(\ell) d\ell$$

$\rho(\ell)$  = the background gas ( $\text{H}_2$ ) density, which is a function of the distance into the gas cell,  $\ell$ .

$$S_1 \equiv \frac{1}{2}C_{01}^{21} + \frac{1}{2}C_{00}^{21} + C_{01}^{22} \quad @ \ 2E/3$$

$$S_2 \equiv \frac{1}{2}C_{11}^{21} + \frac{1}{2}C_{10}^{21} + C_{10}^{22} \quad @ \ 2E/3$$

$$S_3 \equiv \frac{1}{3}C_{11}^{31} + \frac{1}{3}C_{10}^{31} + \frac{2}{3}C_{11}^{32} + \frac{2}{3}C_{10}^{32}$$

$$S_4 \equiv \frac{1}{2}C_{11}^{21} + \frac{1}{2}C_{10}^{21} + C_{10}^{22}$$

$$S_5 \equiv \frac{1}{2}C_{10}^{21} + \frac{1}{2}C_{00}^{21} + C_{01}^{22}$$

$y$  = the ratio of a species number density to the one of each family at  $x = 0$ , the numeral subscript indicating the number of atoms in a molecular species, and (0, +, -) charge states.

$C_{cd}^{ab}$  = reaction cross section involving a mass change from a to b and a charge state change from c to d.

The last equation of each family is simply from the conservation of momentum. The boundary condition for each group is that the original ion fractions ( $y_+$ ,  $y_{2+}$ , and  $y_{3+}$ ) are unity at  $x = 0$  and all the others are zero at  $x = 0$ .

With the boundary condition,  $y_0(0) = 1$ , Eq. (1) also describes the problem of a pure neutral beam of 100% atomic particles traveling a drift tube. If the situation is such that any charged species are deflected out of the beam passage and dumped to the drift tube wall by the influence of the magnetic fields of a plasma confinement device, then  $y_+$  and  $y_-$  will be zero everywhere.

The solutions to the simultaneous differential equations of each family are given below.

$\text{H}^+$  family

$$y_+(x) = A_1 e^{-\alpha_1 x} + A_2 e^{-\alpha_2 x} + A_3, \quad (4)$$

$$y_0(x) = B_1 e^{-\alpha_1 x} + B_2 e^{-\alpha_2 x} + B_3 \quad (5)$$

$$y_-(x) = 1 - y_+(x) - y_0(x) \quad (6)$$

where

$$A_1 = \frac{\alpha_2 A_3 - \alpha_2 + C_{10} + C_{1-1}}{\alpha_1 - \alpha_2}$$

$$A_2 = \frac{-\alpha_1 A_3 + \alpha_1 - C_{10} - C_{1-1}}{\alpha_1 - \alpha_2}$$

$$A_3 = \frac{pC_{-11} + C_{-10}(C_{01} - C_{-11})}{\alpha_1 \alpha_2}$$

$$B_1 = \frac{\alpha_2 B_3 - C_{10}}{\alpha_1 - \alpha_2}$$

$$B_2 = \frac{-\alpha_1 B_3 + C_{10}}{\alpha_1 - \alpha_2}$$

$$B_3 = \frac{qC_{-10} + C_{-11}(C_{10} - C_{-10})}{\alpha_1 \alpha_2}$$

$$\left. \begin{array}{l} \alpha_1 \\ \alpha_2 \end{array} \right\} = \frac{1}{2} \left[ p + q \pm \sqrt{(p - q)^2 + 4(C_{10} - C_{-10})(C_{01} - C_{-11})} \right]$$

$$p = C_{01} + C_{0-1} + C_{-10}$$

$$q = C_{10} + C_{1-1} + C_{-11}$$

H<sub>2</sub><sup>+</sup> family

$$y_{2+}(x) = \frac{C_{10}^{22} C_{01}^{22}}{\beta_1 - \beta_2} \left( \frac{1}{q_1 - s_4} e^{-\beta_1 x} - \frac{1}{q_2 - s_4} e^{-\beta_2 x} \right) \quad (7)$$

$$y_{20}(x) = \frac{C_{10}^{22}}{\beta_1 - \beta_2} \left( -e^{-\beta_1 x} + e^{-\beta_2 x} \right) \quad (8)$$

$$y_0(x) = \frac{2C_{10}^{11}}{C_{10}^{11} + C_{01}^{11}} - \left( \frac{2C_{10}^{11}}{C_{10}^{11} + C_{01}^{11}} + D_1 + D_2 \right) e^{-(C_{10}^{11} + C_{01}^{11})x} + D_1 e^{-\beta_1 x} + D_2 e^{-\beta_2 x} \quad (9)$$

$$y_+(x) = 2(1 - y_{20} - y_{2+}) - y_0 \quad (10)$$

where

$$D_1 = \frac{(S_4 - \beta_2)(C_{10}^{21} - 2C_{10}^{11}) - C_{10}^{22}(C_{00}^{21} - 2C_{10}^{11})}{(\beta_1 - \beta_2)(C_{10}^{11} + C_{01}^{11} - \beta_1)}$$

$$D_2 = \frac{-(S_4 - \beta_1)(C_{10}^{21} - 2C_{10}^{11}) + C_{10}^{22}(C_{00}^{21} - 2C_{10}^{11})}{(\beta_1 - \beta_2)(C_{10}^{11} + C_{01}^{11} - \beta_2)}$$

$$\left. \begin{array}{l} \beta_1 \\ \beta_2 \end{array} \right\} = \frac{1}{2} \left[ S_4 + S_5 \pm \sqrt{(S_4 - S_5)^2 + 4C_{10}^{22}C_{01}^{22}} \right]$$

H<sub>3</sub><sup>+</sup> family

$$y_{3+}(x) = e^{-S_3 x} \quad (11)$$

$$y_{2+}(x) = G_1 e^{-\gamma_1 x} + G_2 e^{-\gamma_2 x} + G_3 e^{-S_3 x} \quad (12)$$

$$y_{20}(x) = H_1 e^{-\gamma_1 x} + H_2 e^{-\gamma_2 x} + H_3 e^{-S_3 x} \quad (13)$$

$$y_0(x) = \frac{3C_{10}}{C_{10} + C_{01}} - \left( \frac{3C_{10}}{C_{10} + C_{01}} + K_1 + K_2 + K_3 \right) e^{-(C_{10} + C_{01})x} + K_1 e^{-\gamma_1 x} + K_2 e^{-\gamma_2 x} + K_3 e^{-S_3 x} \quad (14)$$

$$y_+(x) = 3 - y_0 - 2y_{20} - 2y_{2+} - 3y_{3+} \quad (15)$$

where

$$G_1 = \frac{C_{11}^{32}C_{10}^{22} - C_{10}^{32}(\gamma_1 - S_1)}{(\gamma_1 - \gamma_2)(\gamma_1 - S_3)}$$

$$G_2 = -\frac{C_{11}^{32}C_{10}^{22} - C_{10}^{32}(\gamma_2 - S_2)}{(\gamma_1 - \gamma_2)(\gamma_2 - S_3)}$$

$$G_3 = \frac{C_{11}^{32}C_{10}^{22} - C_{10}^{32}(S_3 - S_2)}{(\gamma_1 - S_3)(\gamma_2 - S_3)}$$

$$H_1 = \frac{C_{10}^{32}C_{01}^{22} - C_{11}^{32}(\gamma_1 - S_1)}{(\gamma_1 - \gamma_2)(\gamma_1 - S_3)}$$

$$H_2 = -\frac{C_{10}^{32}C_{01}^{22} - C_{11}^{32}(\gamma_2 - S_1)}{(\gamma_1 - \gamma_2)(\gamma_2 - S_3)}$$

$$H_3 = \frac{C_{10}^{32}C_{01}^{22} - C_{11}^{32}(S_3 - S_1)}{(\gamma_1 - S_3)(\gamma_2 - S_3)}$$

$$K_1 = \frac{G_1(C_{00}^{21} - 2C_{10}^{11}) + H_1(C_{10}^{21} - 2C_{10}^{11})}{C_{10} + C_{01} - \gamma_1}$$

$$K_2 = \frac{G_2(C_{00}^{21} - 2C_{10}^{11}) + H_2(C_{10}^{21} - 2C_{10}^{11})}{C_{10} + C_{01} - \gamma_2}$$

$$K_3 = \frac{G_3(C_{00}^{21} - 2C_{10}^{11}) + H_3(C_{10}^{21} - 2C_{10}^{11}) + C_{10}^{31} - 3C_{10}}{C_{10} + C_{01} - S_3}$$

$$\left. \begin{matrix} \gamma_1 \\ \gamma_2 \end{matrix} \right\} = \frac{1}{2} \left[ S_1 + S_2 \pm \sqrt{(S_1 - S_2)^2 + 4C_{10}^{22}C_{01}^{22}} \right]$$

Traveling further downstream, the charged particles of the beam are swept away from the neutral particles by a deflection magnet after a gas cell. If the gas cell line density is high enough to provide the equilibrium, essentially all the neutrals entering into a drift region (i.e., the region between the deflection magnet and the plasma device) will be mono-atomic particles in three discrete energy groups (i.e.,  $E$ ,  $E/2$ ,  $E/3$ ). The initial conditions are then set by the asymptotic values of  $y_0$  for each group ( $y_0^\infty$ ). For the case where the energetic charged particles produced along the drift tube are to travel together with the neutral particles, the solutions are in terms of the drift tube line density,  $x$ ,

$$y_+(x') = y_0^\infty \left( R_1 e^{-\alpha_1 x'} + R_2 e^{-\alpha_2 x'} + A_3 \right) \quad (16)$$

$$y_0(x') = y_0^\infty \left( T_1 e^{-\alpha_1 x'} + T_2 e^{-\alpha_2 x'} + B_3 \right) \quad (17)$$

$$y_-(x') = y_0^\infty - y_+(x') - y_0(x') \quad (18)$$

where

$$R_1 = \frac{\alpha_2 A_3 - C_{01}}{\alpha_1 - \alpha_2}$$

$$R_2 = \frac{-\alpha_1 A_3 + C_{01}}{\alpha_1 - \alpha_2}$$

$$T_1 = \frac{\alpha_2 B_3 - \alpha_2 + C_{01} + C_{0-1}}{\alpha_1 - \alpha_2}$$

$$T_2 = \frac{-\alpha_1 B_3 + \alpha_1 - C_{01} - C_{0-1}}{\alpha_1 - \alpha_2}$$

$y_0^\infty$  = the equilibrium fraction of neutrals entering the drift tube.

In the case when the charged particles are lost to the wall at the location where they are born, i.e., if they do not convert themselves into neutrals, the solutions are

$$y_-(x') = y_0 e^{-(C_{01} + C_{0-1})x'} \quad (19)$$

$$y_+(x') = y_0^+ \frac{C_{01}}{C_{01} + C_{0-1}} \left[ 1 - e^{-(C_{01} + C_{0-1})x'} \right] \quad (20)$$

$$y_-(x') = \frac{C_{0-1}}{C_{01}} y_+(x') \quad (21)$$

### 3. CALCULATIONS OF SPECIES EVOLUTION

Using the solutions Eqs. (4)-(15), the fractional power of each species is calculated as a function of the line density for different beam energies (see Figs. 2-7). The fractional powers carried by the species of molecular ion families are estimated from the number fractions ( $y$ 's) weighted by their fractional energies. The equilibrium fractions calculated herein are in fair agreement with the measured data.<sup>3</sup> Appropriate cross sections are tabulated in Table 1. Most cross section values are taken from Ref. 3 and they differ only slightly from the ones compiled by Stearns et al.<sup>2</sup>

In Fig. 8 the surviving fraction of the neutral beam in the drift tube,  $y_0(x')/y_0^\infty$ , is shown as a function of both the line density of the drift tube and the neutral beam energy, where  $y_0^\infty$  is the equilibrium fraction of the neutral beam after the gas cell. It can be seen from Fig. 8 that about 10% loss of neutral beams occurs in the drift tube due to ionizing collisions at the line density of  $10^{15} \text{ cm}^{-2}$  (or  $3 \times 10^{-4} \text{ torr-m}$ ). A runaway situation could exist if the gas line density increases rapidly due to "boil-off" of gas by energetic particles lost to the drift tube wall.<sup>4</sup> The conversion efficiency of ion beam power into neutral beam power is then given by the following expression,

$$\eta_n = \sum_{k=1}^3 \frac{f_k}{k} y_{0,k}(x_0) \exp \left\{ - \left[ C_{01}(E/k) + C_{0-1}(E/k) \right] x_0' \right\}, \quad (22)$$

where  $f_k$  is the fraction of the ion component,  $k$ , in the original ion beam,  $k$  being 1, 2, and 3 for  $H_1^+$ ,  $H_2^+$ , and  $H_3^+$  family, respectively.  $Y_{0,k}(x_0)$  is the fraction of energetic atoms originated from the  $k$  family, evaluated at a gas cell line density of  $x_0$ . The line density of the entire

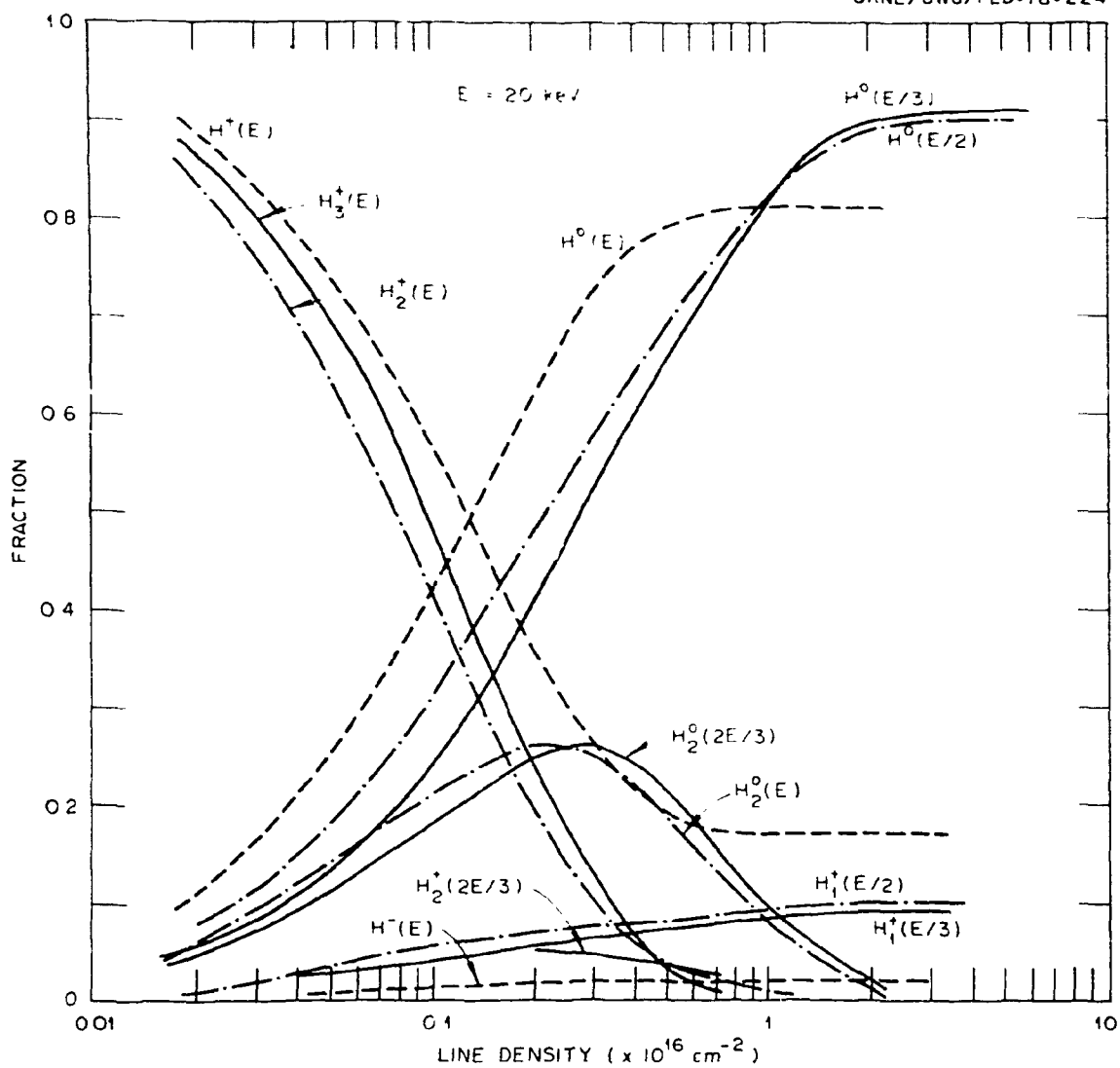


Fig. 2. Variation of fractional powers carried by particle species as a function of the downstream line density of H<sub>2</sub> (or D<sub>2</sub>) for hydrogen energy of 20 keV (or 40 keV for deuterium beams).

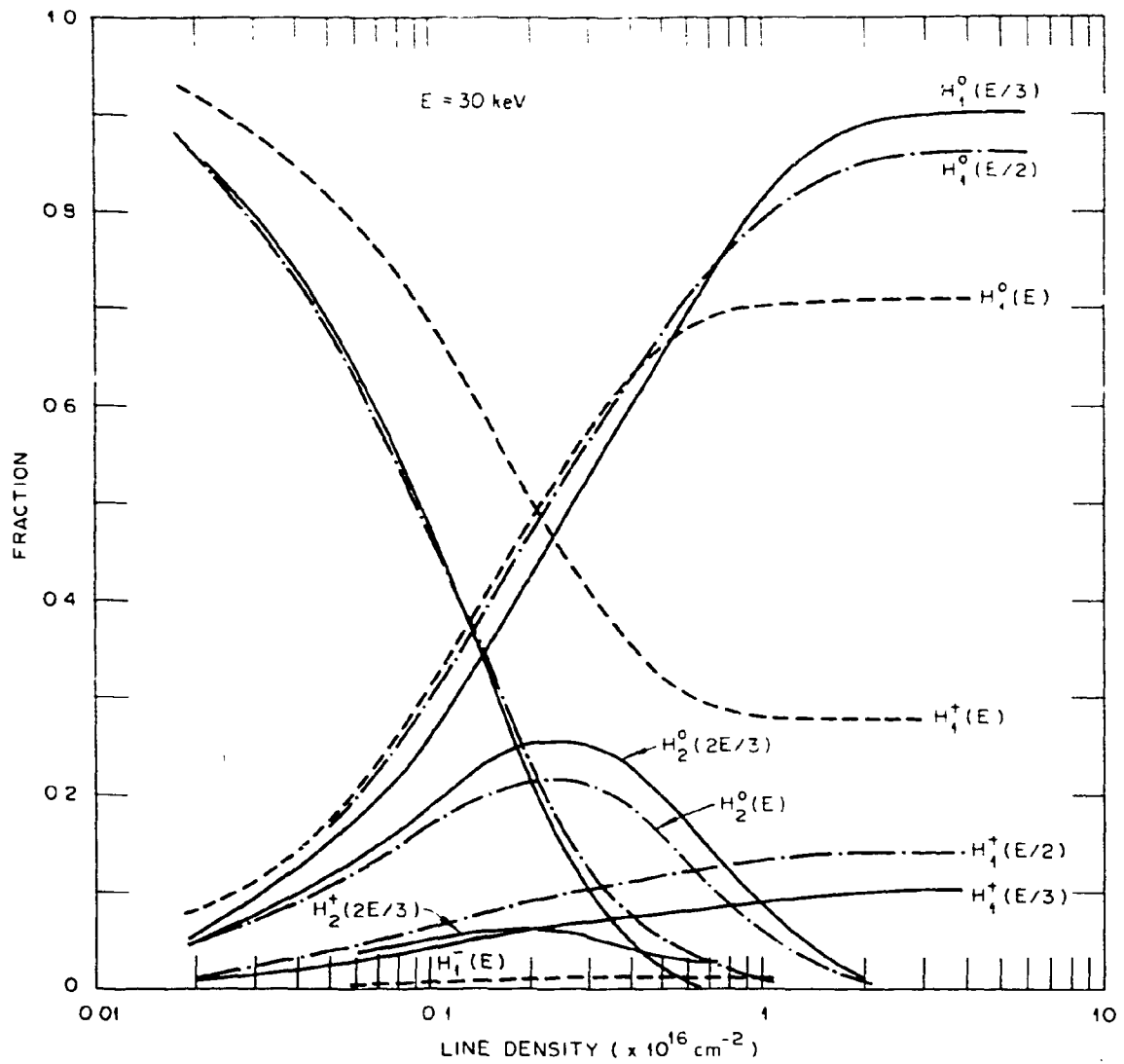


Fig. 3. Variation of fractional powers carried by particle species as a function of the downstream line density of H<sub>2</sub> (or D<sub>2</sub>) for hydrogen energy of 30 keV (or 60 keV for deuterium beams).



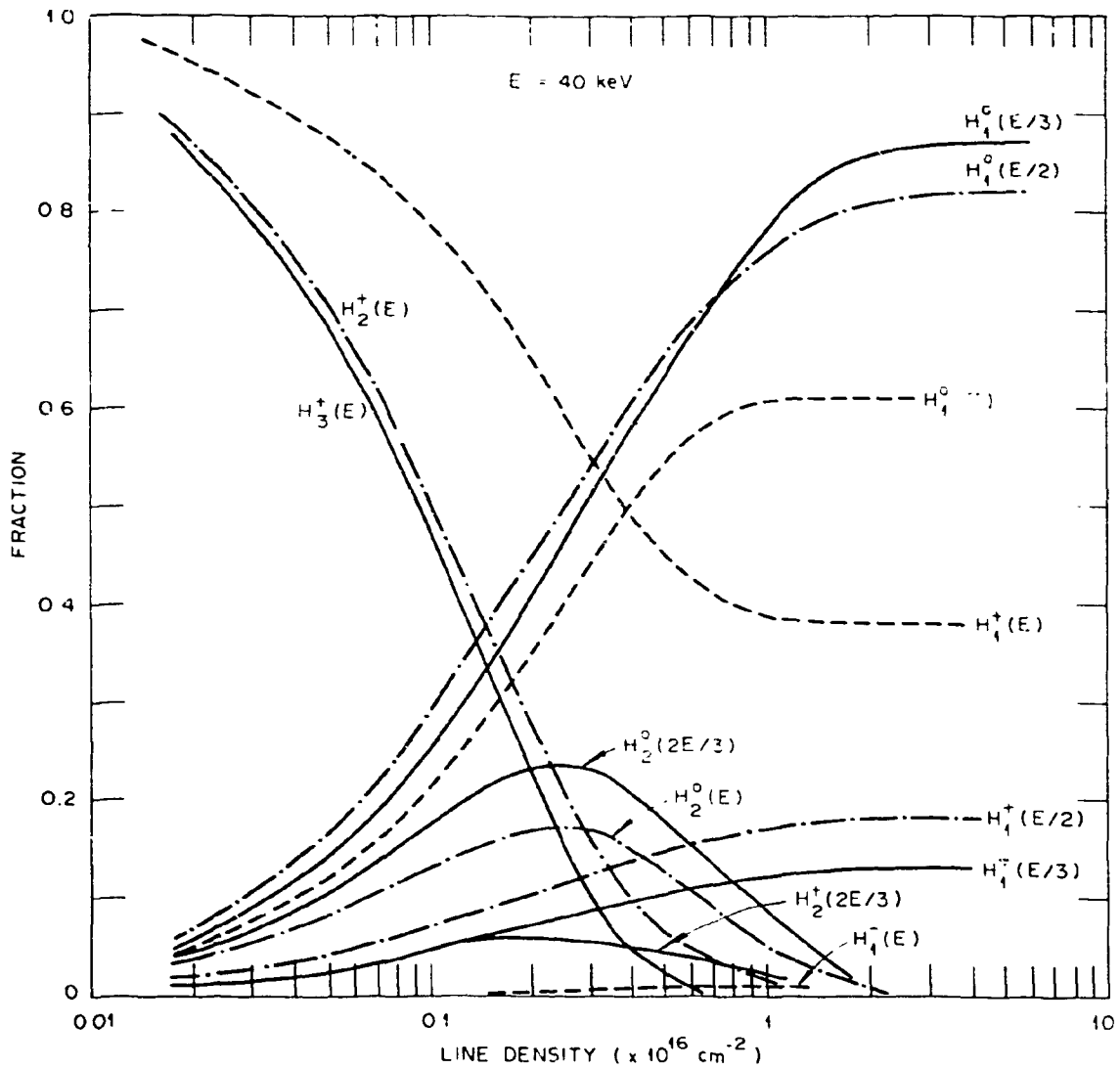


Fig. 4. Variation of fractional powers carried by particle species as a function of the downstream line density of H<sub>2</sub> (or D<sub>2</sub>) for hydrogen energy of 40 keV (or 80 keV for deuterium beams).

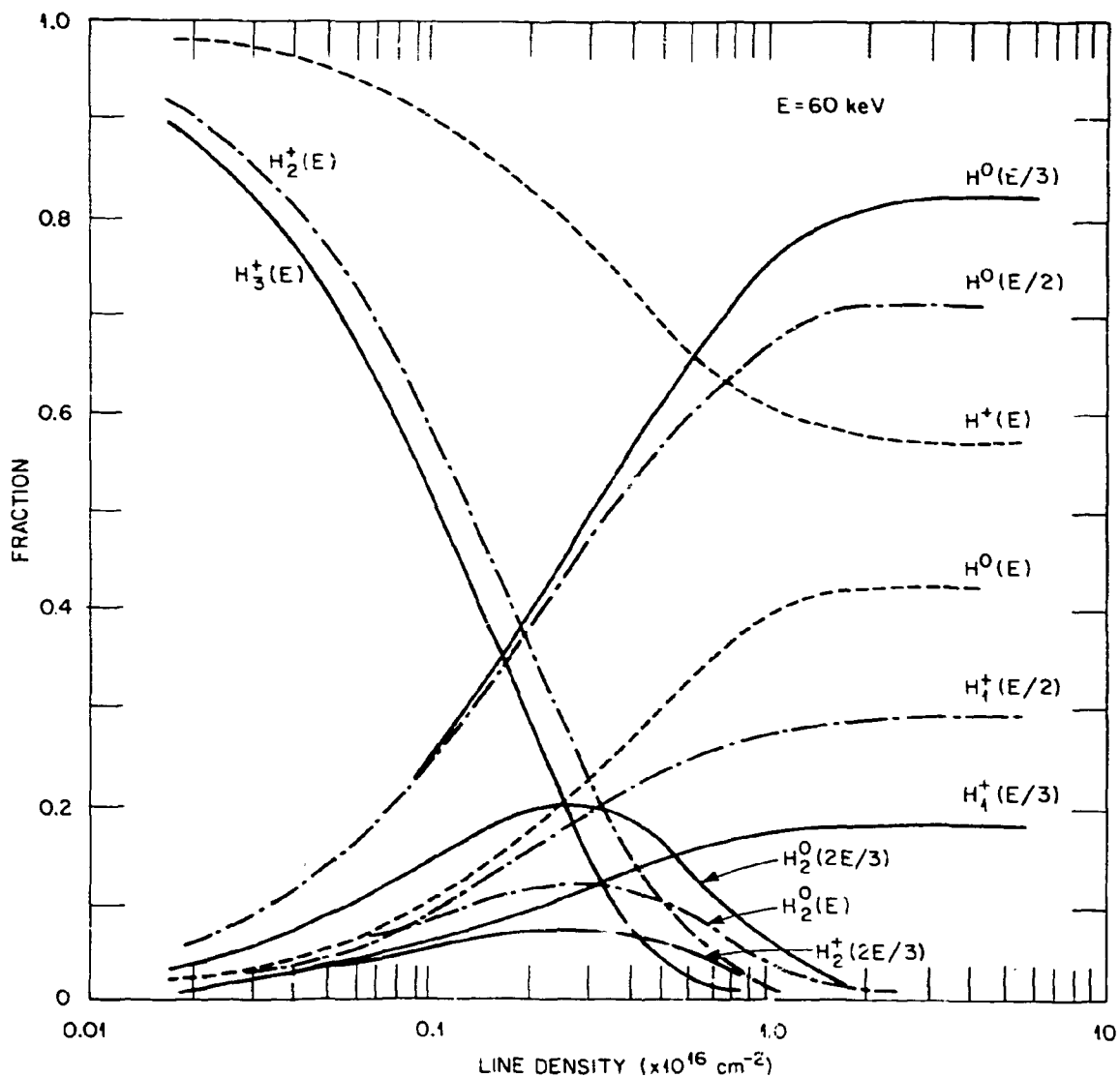


Fig. 5. Variation of fractional powers carried by particle species as a function of the downstream line density of H<sub>2</sub> (or D<sub>2</sub>) for hydrogen energy of 60 keV (or 120 keV for deuterium beams).

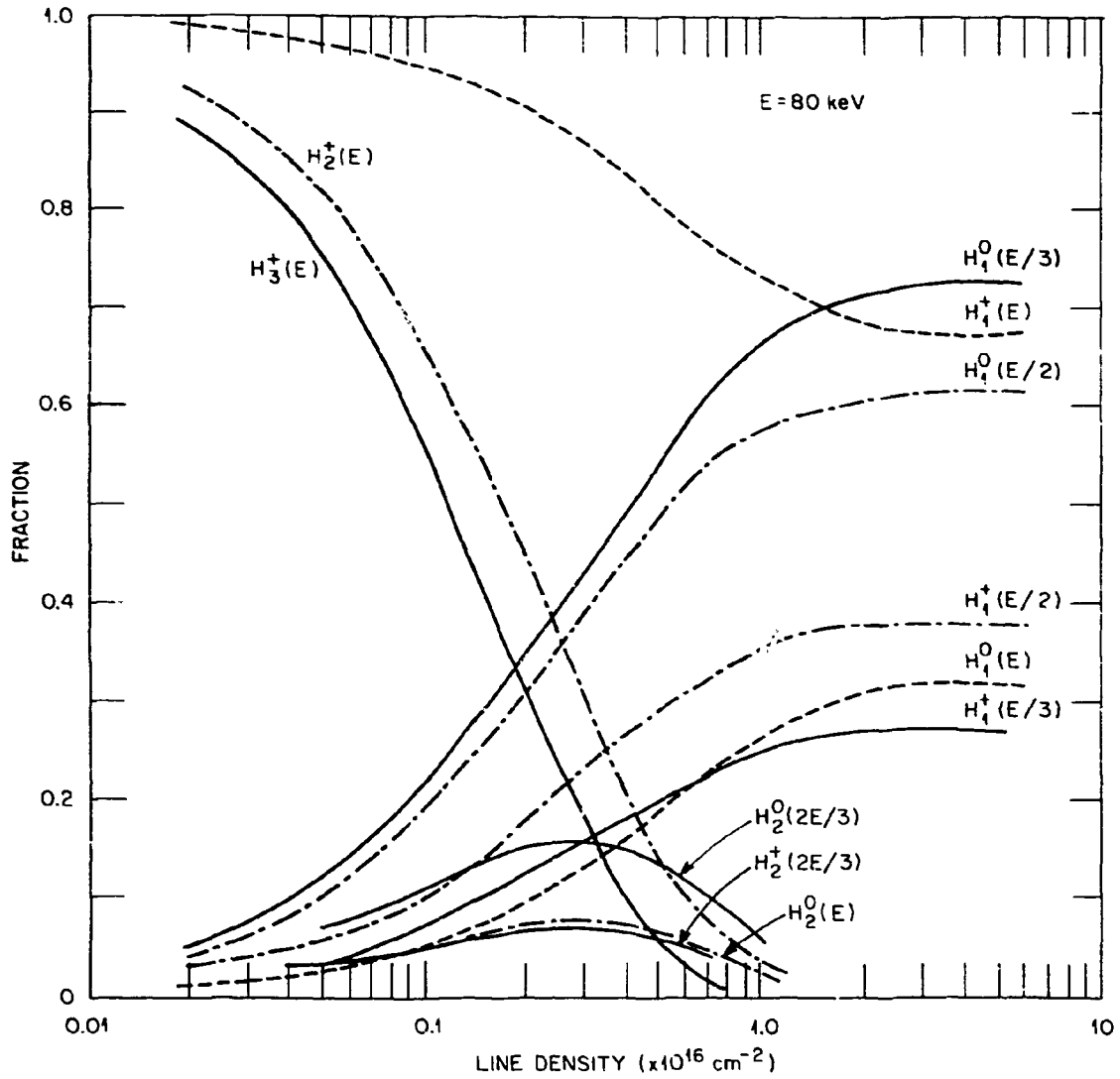


Fig. 6. Variation of fractional powers carried by particle species as a function of the downstream line density of H<sub>2</sub> (or D<sub>2</sub>) for hydrogen energy of 80 keV (or 160 keV for deuterium beams).

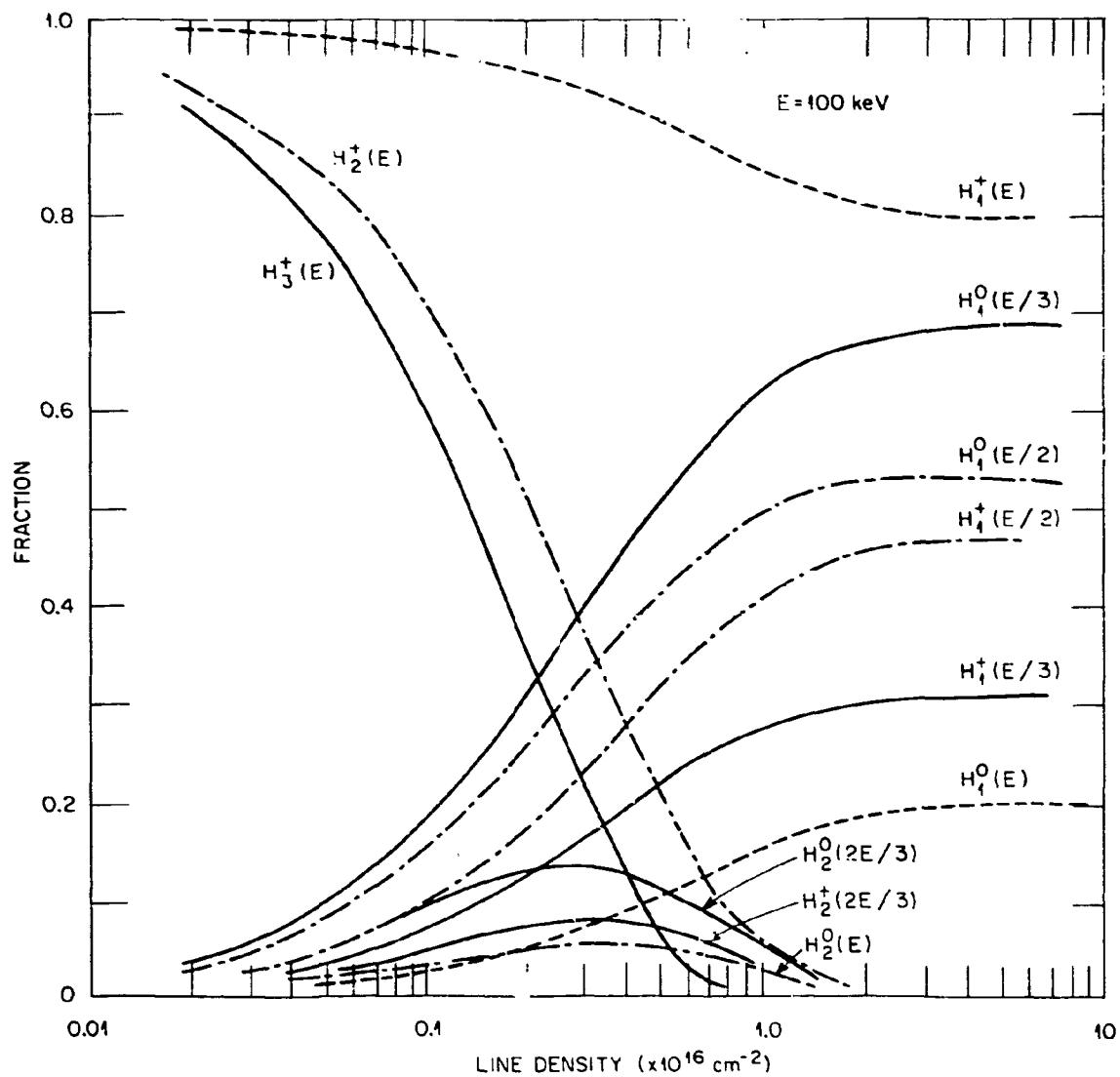


Fig. 7. Variation of fractional powers carried by particle species as a function of the downstream line density of  $H_2$  (or  $D_2$ ) for hydrogen energy of 80 keV (or 200 keV for deuterium beams).

Table 1. Cross sections (in units of  $10^{-16}$  cm<sup>2</sup>) used for the species calculations compiled from Ref. 3

Ion energy (keV)	$C_{10}^{11}$	$C_{01}^{11}$	$C_{1-1}^{11}$	$C_{0-1}^{11}$	$C_{-11}^{11^a}$	$C_{-10}^{11^a}$	$C_{10}^{22}$	$C_{01}^{22}$	$C_{01}^{21^b}$	$C_{00}^{21^a}$	$C_{11}^{21^a}$	$C_{10}^{21}$	$C_{11}^{32}$	$C_{10}^{32}$	$C_{11}^{31}$	$C_{10}^{31}$
10	8.5	0.92	0.047	0.22	0.4	10.0	4.6	0.67	0.38	2.4	2.4	7.7	1.1	3.4	0.86	6.2
20	6.0	1.3	0.1	0.19	0.44	8.7	3.6	1.2	0.43	1.98	2.1	8.5	1.25	4.1	1.65	8.8
30	4.0	1.6	0.062	0.12	0.44	7.4	2.8	1.5	0.6	1.63	1.9	8.2	1.3	4.3	1.8	9.6
40	2.6	1.6	0.025	0.095	0.43	6.7	2.1	1.7	0.67	1.28	1.9	7.7	1.25	4.1	1.95	9.6
60	1.1	1.5	0.0022	0.053	0.4	5.4	1.2	1.8	0.67	1.0	2.2	6.1	1.15	3.15	2.15	9.0
80	0.56	1.2	0.0005	0.029	0.34	4.7	0.7	2.0	0.49	0.85	2.4	4.6	1.1	2.4	2.3	7.9
100	0.28	1.1	0.0001	0.021	0.30	4.0	0.45	2.0	0.3	0.75	2.3	3.6	0.99	1.9	2.3	6.7
120	0.15	0.95	0.00003	0.008	0.25	3.6	0.3	2.0	0.3	0.67	2.25	2.5	0.92	1.6	2.3	5.2

<sup>a</sup>Considerable deviations observed between Ref. 2 and Ref. 3.

<sup>b</sup>Taken from Ref. 2.

ORNL/DWG/FED-78-219

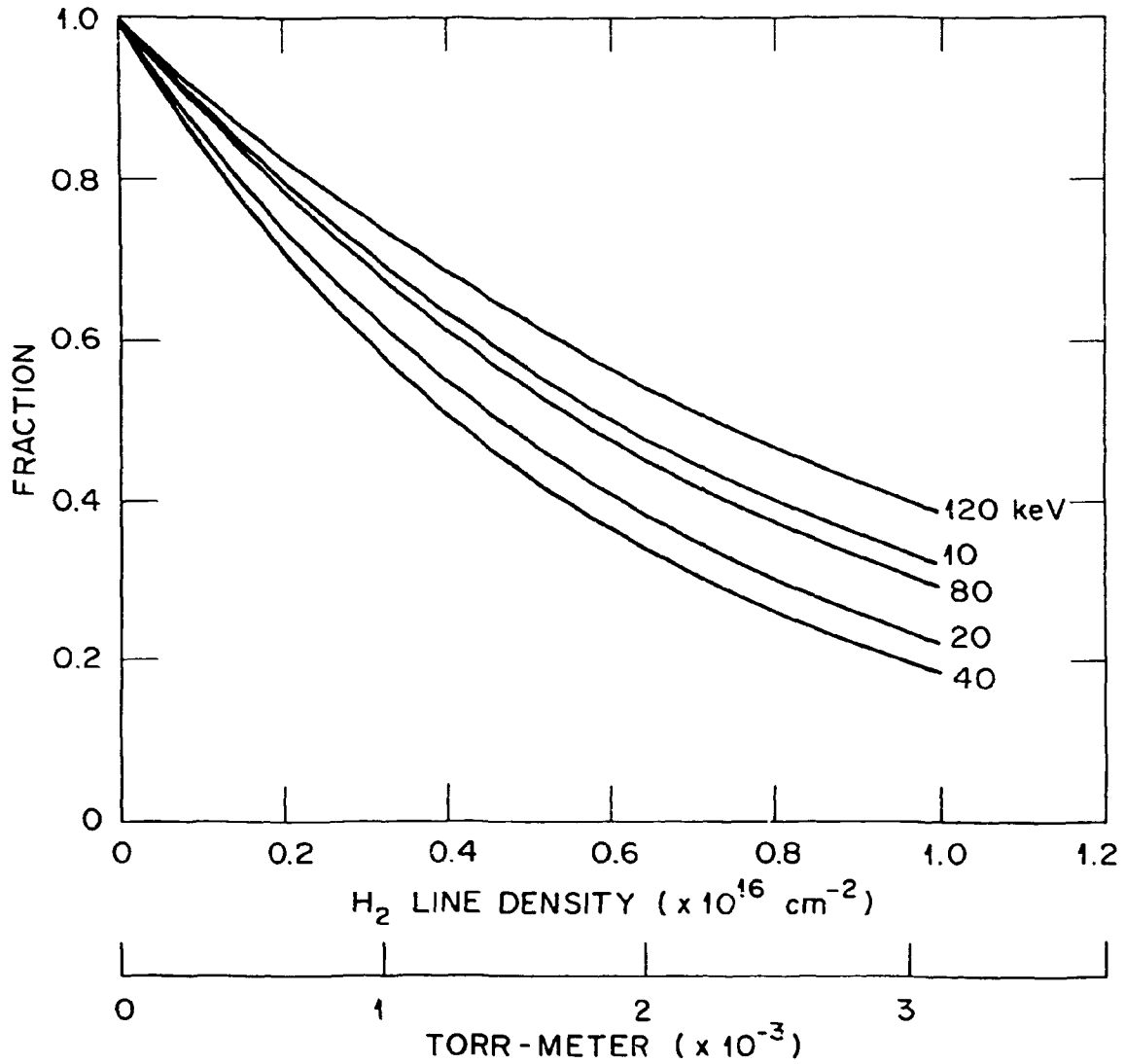


Fig. 8. The surviving fraction of atomic hydrogen beam as a function of the drift tube line density ( $H_2$ ) and the neutral beam energy.

drift tube is denoted by  $x_0'$ . The gas cell line density,  $x_0$ , is usually set less than the equilibrium line density in a neutral beam injection system, since the fraction of neutrals is a slow function of the line density near the equilibrium, and achieving the equilibrium line density is at the expense of large vacuum pumping power.

#### 4. CALCULATIONS OF NEUTRAL BEAM POWER

Positive hydrogen ion beams are potentially inefficient at high energy since the neutralization efficiency decreases with the beam energy. The conversion efficiency given by Eq. (22) and Figs. 2-7 at a given gas cell and drift tube condition provides the information needed for neutral beam injection systems design.

Another useful way to present the problem of neutralization is to plot the neutral power as a function of beam energy for a fixed beam current. Since the extractable ion beam current is limited due to considerations of optics and breakdown voltage, there is a practical upper limit on the extraction current density. Thus far, all the neutral beam injector sources have yielded average current densities in the range between 0.3 and 0.4 A/cm<sup>2</sup>. The total current from a source has been simply scaled up by the increase of the emitting area. However, there would be a limit on the size of an ion source due to the difficulty of maintaining the source gas pressure differential and the source plasma uniformity. Consequently, it is well justified to assume that an ion source as presently designed is current limited.

In this respect, Fig. 9 shows the neutral beam power per ampere of ion beam as a function of both the beam energy and the species distribution. (The  $H_3^+$  component is neglected for simplicity.) The gas cell line density is chosen such that 90% of the equilibrium fraction is to be achieved for  $H_1^+(E)$ . For simplicity, the loss along the drift tube is neglected. The actual power realized at the fusion plasma per ampere of ion current is the product of the neutral power shown in Fig. 9, the overall geometric transmission efficiency (due to beam divergence),<sup>5</sup> and the surviving fraction of the neutral beam in passing through the drift tube (Fig. 8). The power carried by the half energy component is the sum of  $H_1^0(E/2)$  and  $H_2^0(E)$ , although above 80 keV, the  $H_2^0(E)$  component becomes negligible.

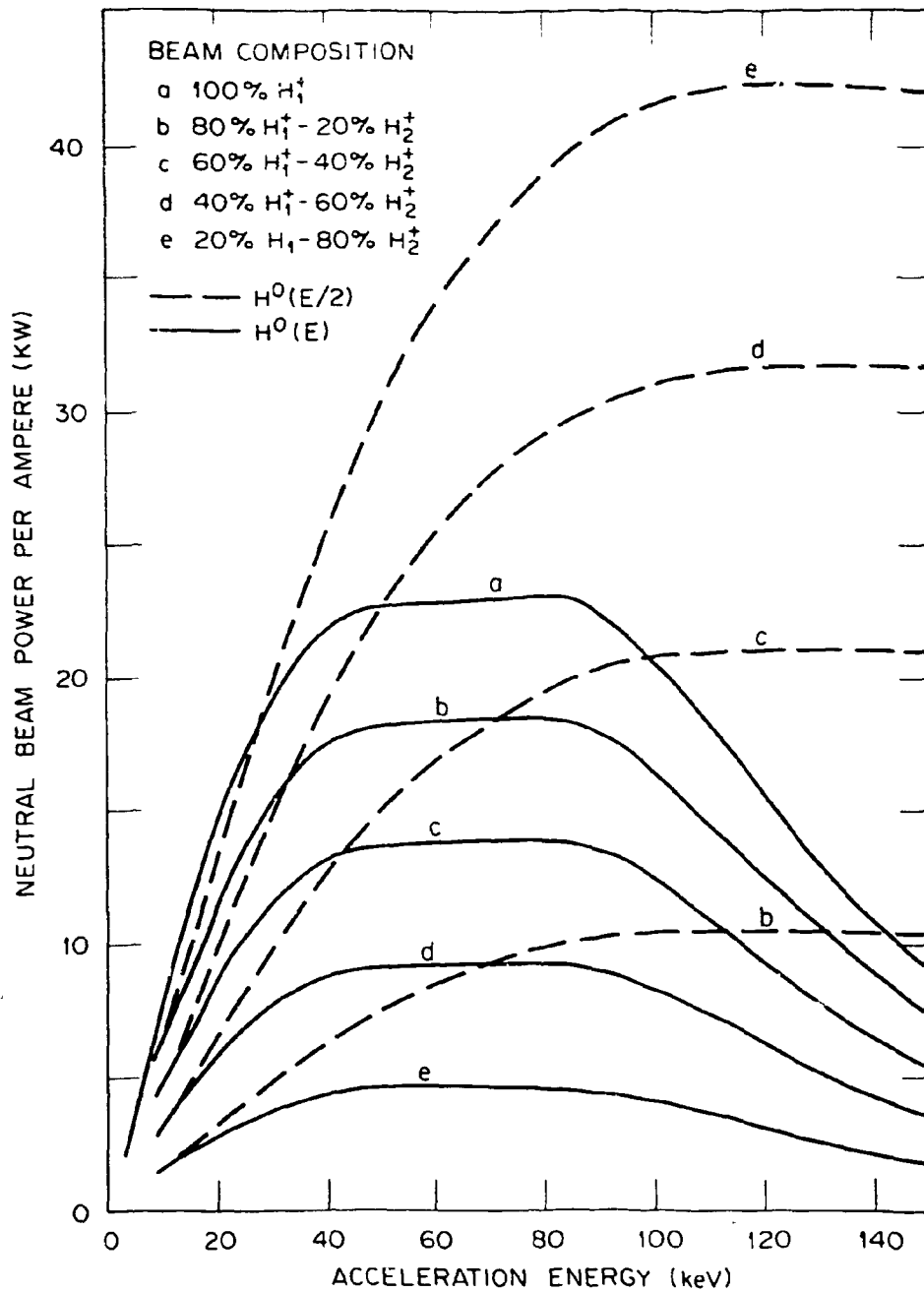


Fig. 9. Neutral beam powers per ampere of the original ion beam current as a function of the beam energy for different species distributions ( $H_1^+$  and  $H_2^+$  only). For each energy the line density for the 90% equilibrium for  $H^+(E)$  is used.



One can notice from Fig. 9 that the neutral beam power carried by the full energy particles has an apparent maximum with respect to the beam energy. A maximum plateau appears in the energy range between 40 and 80 keV. The current neutral beam program is in this energy range, e.g., 40 keV  $H^0$  for PLT, 120 keV  $D^0$  (60 keV  $H^0$  equivalent) for TFTR, and others. One also notices that in this energy range the efficiency varies as the inverse of the energy. The beam energy, at which the total neutral power (both half- and full-energy particles) is maximum, varies according to the species composition, from  $\sim 70$  keV for 100%  $H_1^+$ ,  $\sim 80$  keV for 60%  $H_1^+$ -40%  $H_2^+$ , to  $\sim 100$  keV for 20%  $H_1^+$ -80%  $H_2^+$ .

## 5. CONCLUSIONS

We have presented analytic solutions to the rate equations for ion-molecule interactions in a gas cell and a drift tube. Evolution of species as a function of line density was given for a wide range of energy of interest to neutral beam injection heating of fusion plasma (20-100 keV per nucleon). It should be noted that the compiled cross sections typically have standard deviations of  $\pm 20$ -40%. The neutral beam power per unit ion beam current was also calculated as a function of the ion beam energy, elucidating the maximum obtainable neutral beam powers. The neutral beam power per ampere of ion current is more or less constant in the energy range between 40 and 80 keV for atomic hydrogen ions.

## ACKNOWLEDGMENT

We gratefully acknowledge L. D. Stewart and J. H. Whealton for useful suggestions and discussions.

## REFERENCES

1. K. H. Berkner, R. V. Pyle, and J. W. Stearns, *Nucl. Fusion* 15, 249 (1975).
2. J. W. Stearns, K. H. Berkner, and R. V. Pyle, *Proc. 2nd Topical Meeting on the Technology of Controlled Nuclear Fusion*, Vol. IV, p. 1221 (1976).
3. C. F. Barnett et al., *Atomic Data for Controlled Fusion Research*, ORNL-5206 and ORNL-5207, Oak Ridge, Tennessee (1977).
4. A. C. Riviere and J. Sheffield, *Nucl. Fusion* 15, 944 (1975);  
L. D. Stewart, private communication; W. K. Dagenhart et al., ORNL/TM-6374, Oak Ridge, Tennessee (1978).
5. J. Kim and J. H. Whealton, *Nucl. Instrum. Methods* 141, 187 (1977).